Influence of magnetic field and radiation on heat and mass transfer flow of nano fluid over an inclined vertical plate embedded in porous medium

P Yogeswara Reddy[a], Dr G S S Raju[b]

[a] Department of Mathematics, Vemana Institute of Technology, Bengaluru, Karnataka, India
[b] Department of Mathematics, JNTU college of Engineering, Pulivendula, YSR dist,A P, India

Article History: Received: 10 January 2021; Revised: 12 February 2021; Accepted: 27 March 2021; Published online: 28 April 2021

Abstract: We have analyzed MHDboundary layer flow, heat and mass transfer analysis of nanofluid over an inclined vertical plate saturated by porous medium with thermal radiation, and heat generation/absorption. Suitable similarity variables are introduced to convert non-linear partial differential equations into ordinary differential equations and these equations together with associated boundary conditions are solved numerically by using versatile, extensively validated, variational Finite element method. The impact of various pertinent parameters on hydrodynamic, thermal and concentration boundary layers are examined in detail and the results are shown graphically. Furthermore, the impact of these parameters on local skin friction coefficient, rate of heat transfer andrate of mass transferis also investigated. The results are compared with the works published previously and found to be excellent agreement.

Keywords: MHD, nano fluid, embedded, Skin friction

1. Introduction

The convectional heat transmits fluids like water, ethylene glycol and oilhavelow temperature relocation-movement abilities owed to their less thermal-heat movement. To get better the heat-thermal transportation of these flowfluids (10^{-9})nano/micro-sizedparticle equipment be balanced in fluids/liquids. quite a few speculative as well as investigational reseaches contains are prepared to boost the heat/thermal transportations of these fluids; hoi [1] be the foremost along with all who Showcased a fresh category of liquid called naanofluid's at the same time as study on fresh cooling agents with cooling expertise. Eastmen etal[2] This be for the rationale so as to escalating exterior region of the support solution duo to the deferment of nanoparticales. Esttman etal [3] cover as well be evidenced for so as to the heat/thermal transportation was amplified forty percent while copper nanoparticles of quantity portion a smaller amount than one percent are extra to the etylene glicol or oil. Choi et al. [4] encompass to facilitate here is one hundred and fifty percent development in heat/thermal transportation from one end to other while carbon nano pipes are supplementary to the ethilene glicol or oil. on top, Xie et al. [5] encompass Al_2O_3- ethyline glicol based nanoliquid flows heat/thermal transportation is amplified in the assortment twenty five to thirty percent while Alumina nanoparticales are included. The enhancement in heat/tharmal transportaion of this enormity is not merely relay on elevated heat/thermel movement characteristics of the included substances of nano nature other than as well inclined to numerous additional mechanisams like extent of substances, constituent part agglomeration, quantity portion of the nanoatoms, Brownian proposition, substance extent, thermophorasys and so on. It is seen by numerous investigater credentials in writing which arranges the warmth and collection transfer distinctiveness of naanofluids by making an allowance for Brownian proposition and thermophoresis possessions into version. Recently, Nield and Kuznetsov[6]comprise conversed the Ching-Mincowycz dilemma for normal convection boundarylayer stream in a permeable intermediate drenched nanoo solution. Kuznetsov&Nield[7] premeditated the manipulate of Brownian, shift in addition to thermophoresison ordinary convection border line sheet stream of a naano solution history a upright shield. Khan&pop [8] comprise of discussion border line film flow of a naano solution precedent a widen sheet. Chamkha etal[9] premeditated the diverse convectionMHD stream of a nanoo solution history a elongated permeable plane during the occurrence of Brownian shift and thermophoresis possessions.

Magnetic field has many applications metallurgical process such as drawing, annealing and tinning of copper wires involve cooling of continuous strips or filaments by drawing them through a quotient fluid. In this process the properties of the final product can effect, so, the rate of cooling can be controlled by using an electrically conducting fluid and the magnetic field applications.In chemotherapy process, concentratingthe drug on the area of interest (tumor site) is done by binding established anticancer drugs with magnetic nanoparticles (Ferrofluids). On the other hand, the thermal emission consequence resting on assorted convection warmth relocation during permeable medium is incredibly vital during elevated hotness progression as well as space expertise as well as has lots of imperative claims such as legroom knowledge, as well as progression concerning elevated hotness such as geo thermal engineering, the reasonable warmth cargo space bed, the nuclear reactor cooling structure and subversive nuclear wastes discarding. Yih[13, 14] premeditated emission consequence on assorted convection more than an isothermal wedgie/cone within permeable medium. Bakier[15] offered an scrutiny of the thermal emission consequence on immobile assorted convection as of upright surfaces in drenched permeable medium. Kumari&Nath[16] premeditated the emission consequence on the nonDarcy assorted convection stream above a nonisothermal flat exterior within a permeable middling.

The setback of border line deposit, high temperature as well as collection relocate movements from first to last permeable intermediate in excess of an disinclined laminate has acknowledged a good deal notice within fresh time as of it's manufacturing as well as industrialized usage of conceptas. Chamka etal. [20] Comprised the likely movement beginning on liable shield from first to last a changeable porosity permeable middling among compelling pasture as well as cosmological energy. Also recommended with the intention of escalating the shield proclivity slant defy the proposition of the solution which results an development in the hotness of the solution. Alam.etal. [21] has premeditated the collision ofheat making and thermophoresisover a half-infynite leaning shield by pleasing captivating pasture addicted to the version. exceptionally a moment ago, PuneetRana et al. [22] comprise accessible restricted component and limited disparity statistical explanation for diverse convection stream of a nanofluid the length of a semiinfinite tending plane shield as of end to end permeable middling in the occurrence of Brownian proposition and thermophoresis and concluded with the aim of hotness and focus side views has been outstandingly prejudiced by way of shield penchant constraint.

In the direction of the preeminent of instigator acquaintance, rejection learning's of descripted that in the prose toward converse MHD mixed convection warmth as well as gathering relocate distinctiveness of a nanoo solution saturated porous middling larger than an inclined upright flat plate in the presence of thermal energy emission as well as warmth making/assimilation. that's why, we completed an endeavor on the way to converse the predicament now. The malformed conservation equations together with border line state of affairs are resolved statistical by by means of an optimized, classical and most validated finite element method.

2. Geometric study

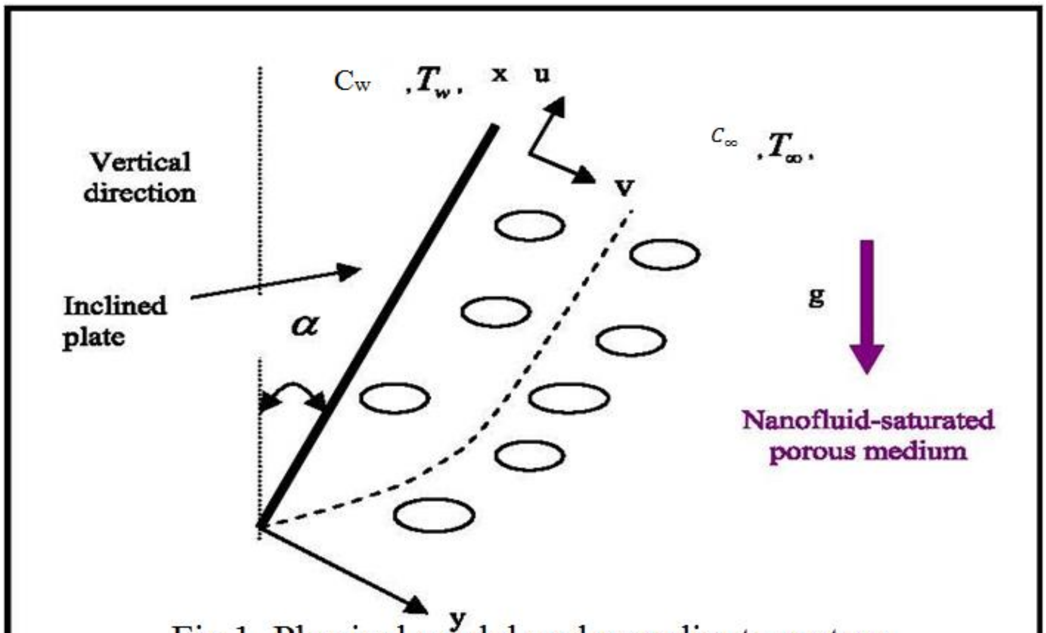

Fig.1. Physical model and coordinate system

think about stable, laminar, 2 way, non shrinkable, diverse get-together stream in excess of a semiinfinite tending porousflat shield packed with 10^{-9}sized solution, which made an-acute viewpoint α in the direction of the upright, as drawn in Fig.1. T_w, as well as $C_w$are hotness and concentration of shield exterior, andT_∞ as well asC_∞ areambient hotness as well as attention. The stream is alleged to be restricted in a province $y > 0$. We think about the not similar inner warmth starting place/be submerged in the stream to get the hotness and attention differences amid the exterior and the ambeint solution. Keep reference on the position mechanism of Nield and Kazanetsov [6], by making use of the Oberbeck,Boussinesq estimation, the prevailing eqns recitation the stream acquire the consequent superficial appearance

$$\frac{\partial u}{\partial x}+\frac{\partial v}{\partial y}=0 \quad (1)$$

$$\frac{\partial p}{\partial y} = 0 \quad (2)$$

$$\mu_f \frac{1}{\kappa} u = -\frac{\partial p}{\partial x} + g\left[(1 - C_\infty)\rho_{f\infty}\beta(T - T_\infty) - (\rho_p - \rho_{f\infty})(C - C_\infty)\right]\cos\alpha - \frac{\sigma\beta_o^2}{\rho_f} u \quad (3)$$

$$\left(u\frac{\partial T}{\partial x} + v\frac{\partial T}{\partial y}\right) = \frac{k_m}{(\rho c)_f}\frac{\partial^2 T}{\partial y^2} + \frac{\varepsilon(\rho c)_p}{(\rho c)_f}\left[D_B \frac{\partial C}{\partial y}.\frac{\partial T}{\partial y} + \left(\frac{D_T}{T_\infty}\right)\left(\frac{\partial T}{\partial y}\right)^2\right] - Q(T - T_\infty) - \frac{1}{(\rho c)_f}.\frac{\partial}{\partial y}(q_r) \quad (4)$$

$$\frac{1}{\varepsilon}\left(u\frac{\partial C}{\partial x} + v\frac{\partial C}{\partial y}\right) = D_B \frac{\partial^2 C}{\partial y^2} + \left(\frac{D_T}{T_\infty}\right)\frac{\partial^2 T}{\partial y^2} \quad (5)$$

In support on to the predicament explanation areboundary conditions develop into

$$v = 0, \quad T = T_w, \quad C = C_w \quad at \quad y = 0 \quad (6)$$

$$u = U_\infty, \quad T \longrightarrow T_w, \quad C \longrightarrow C_\infty \quad at \quad y = \infty \quad (7)$$

as of eqns (second)(2) as well as (third)(3) by cross-differentiation$p$ possibly will be reduced.

The flow occupation ψ called the same as

$$u = \frac{\partial \psi}{\partial y}, \qquad v = -\frac{\partial \psi}{\partial x} \quad (8)$$

via inserting eqn(8) in eqn(3) to(5), the result may arrive at

$$\frac{\partial^2 \psi}{\partial y^2} = \left[\frac{(1 - C_\infty)\rho_{f\infty}\beta g k}{\mu}\frac{\partial T}{\partial y} - \frac{(\rho_p - \rho_{f\infty})g k}{\mu}\frac{\partial C}{\partial y}\right]cos(\alpha) - \frac{\sigma\beta_o^2}{\rho}\frac{\partial \psi}{\partial y} \quad (9)$$

$$\frac{\partial \psi}{\partial y}\frac{\partial T}{\partial x} - \frac{\partial \psi}{\partial x}\frac{\partial T}{\partial y} = \frac{k_m}{(\rho c)_f}\frac{\partial^2 T}{\partial y^2} + \frac{\varepsilon(\rho c)_p}{(\rho c)_f}\left[D_B \frac{\partial C}{\partial y}\frac{\partial T}{\partial y} + \left(\frac{D_T}{T_\infty}\right)\left(\frac{\partial T}{\partial y}\right)^2\right] - Q(T - T_\infty) - \frac{1}{(\rho c)_f}\frac{\partial}{\partial y}(q_r) \quad (10)$$

$$\frac{1}{\varepsilon}\left(\frac{\partial \psi}{\partial y}\frac{\partial C}{\partial x} - \frac{\partial \psi}{\partial x}.\frac{\partial C}{\partial y}\right) = D_B \frac{\partial^2 C}{\partial y^2} + \left(\frac{D_T}{T_\infty}\right)\frac{\partial^2 T}{\partial y^2} \quad (11)$$

The subsequent comparison conversions be pioneered to make simpler the arithmetical study of the difficulty

$$\eta = \frac{y}{x} Pe_x^{1/2}, \qquad f(\eta) = \frac{\psi}{\alpha_m Pe_x^{1/2}}, \qquad \theta(\eta) = \frac{T - T_\infty}{T_w - T_\infty}, \quad \phi(\eta) = \frac{C - C_\infty}{C_w - C_\infty} \quad (12)$$

Where, $\alpha_m = \frac{k_m}{(\rho c)_f}$.

Theradiative heat flux q_r defined as

$$q_r = -\frac{4\sigma^*}{3K^*}\frac{\partial T^4}{\partial y}, \quad (13)$$

The phrase $T^4$is getting higher within a Taylor chain in relation to T_∞ seeing that follows,

$$T^4 = T_\infty{}^4 + 4T_\infty{}^3(T - T_\infty) + 6T_\infty{}^2(T - T_\infty)^2 + \cdots \quad (14)$$

Within the said eqn(14) ignore superior sort stipulations away from the initial scale within $(T - T_\infty)$, we acquire

$$T^4 \cong 4T_\infty{}^3 T - 3T_\infty{}^4 . \quad (15)$$

Accordingly making use of eqn(15) in eqn(13), we acquire

$$q_r = -\frac{16T_\infty{}^3\sigma^*}{3K^*}\frac{\partial T}{\partial y}. \quad (16)$$

by means of eqns (12)&(16), the eqn $(9) - (11)$ becomes

Momentum border line sheet equn

$$f'' = \frac{Ra_x}{Pe_x}(\theta' - Nr\,\varphi')Cos(\alpha) + Mf' \quad (17)$$

Thermal boundary layer equation:

$$\left(1 + \frac{4}{3}An\right)\theta'' + \frac{1}{2} f\,\theta' + Nb\,\theta'\varphi' + Nt(\theta')^2 - Q\theta = 0 \quad (18)$$

focus (variety dissemination) border line sheet equn

$$\varphi'' + \frac{1}{2}\ Le\ \varphi' + \frac{Nt}{Nb}\theta'' = 0 \quad (19)$$

The altered border line state of affairs be

$$\eta = 0, \quad f = 0\ ,\ \theta = 1\ , \quad \phi = 1.$$

$$\eta \longrightarrow \infty, \ f' = 1\ ,\ \theta = 0\ , \quad \phi = 0. \quad (20)$$

The parameters are

$$Nr = \frac{(\rho_p - \rho_{f\infty})(C_w - C_\infty)}{\rho_{f\infty}\beta(T_w - T_\infty)(1 - C_\infty)}, \quad Nb = \frac{\varepsilon\beta(\rho c)_p D_B(C_w - C_\infty)}{(\rho c)_f\ \alpha_m}, Nt = \frac{\varepsilon(\rho c)_p D_T(T_w - T_\infty)}{(\rho c)_f\ \alpha_m T_\infty}$$

$$Le = \frac{\alpha_m}{\varepsilon D_B},\ Ra_x = \frac{(1 - C_\infty)Kg\beta\rho_{f\infty}(T_w - T_\infty)x}{\mu\alpha_m}\ ,\ Pe_x = \frac{U_\infty x}{\alpha_m},$$

$$Ra = \frac{Ra_x}{Pe_x}, \quad Q = \frac{x^2}{Pe_x\alpha_m}, \quad An = \frac{4T_\infty{}^3\sigma^*}{K^*\alpha_m}, \quad M = \frac{\sigma\beta_o^2 x}{\rho Pe_x^{1/2}}.$$

The non-dimensionl rate of hotness as well as focus be

$$Nu_x = \frac{xq_w}{k(T_w - T_\infty)}, \qquad Sh_x = \frac{xq_m}{D_B(C_w - C_\infty)} \quad (21)$$

On simplification, we get

$$(Pe_x)^{-1/2}Nu_x = -\theta'(0),\ (Pe_x)^{-1/2}Sh_x = -\phi'(0), \quad (22)$$

In the current circumstance, $(Pe_x)^{-1/2}Nu_x\ and\ (Pe_x)^{-1/2}Sh_x$ be submit to as the condensed Nusselt number and condensed Sherwood statistics which are represented by $-\theta'(0)\ and\ -\phi'(0)$ correspondingly.

3. Statistical technique of explanation

The distorted nonlinear eqns (17)–(19) be analysed arthamatically by by means of FEM (23,24,25,26).

4. Outcomes as well as conversation

The swiftness, hotness as well as focus spreadness for different relevant parameters are plottedin diagrams 2to28. The consequences are tallied with for $Nu_x$and Sh_xmeant for a variety of standards of *Nt*and *Nb*with PuneetRana et,al [22] by setting up the supplementary parameters, and be obtainable in chart 1 as well as established superior conformity.

Swiftness summarys of the solution depreciate in the solution system as the ideals of *M* rises as well as been exposed in stature2. On the other hand, in assistance hotness and focus profiles rise through mounting ideals of *M*as drawn in stature3&4. The dissimilarity within swiftness, warmth as well as focus allocations for dissimilar ideals of the shield leaning viewpoint (α) is illustrated in shape5-7. It is observed as of drawing5 so as to through an amplify in the ideals of α in presence is downgrading in the swiftness side view right through the explanation command. It is seen as of drawing6 so as to, by means of an amplify in the shield leaning viewpoint (α) enhances the hotness of the solution. This is since of the reality with the intention of growing values of α stand firm the shift of the solution makes downgrading in the momentum border line sheet width, but, augmentation in the width of the thermal border line sheet. Additionally the deliberation allocation s is amplified among mounting ideals of α in the solution section as in Drawing 7.

The impact of *Nb* resting on swiftness, hotness and focus rise's is exemplified in drawing 8-10. It is examined to make possible an amplify in *Nb*increases the swiftness side views in the solution section, drawing8. The hotness summary of the solution enhanced through the escalating ideals of *Nb*as revealed in drawing9. How ever, the focus side views decrease in value in the solution system by means of augmenting ideals of *Nb*(drawing.10). This kind of propensity in heat and focus is equal since in the case of all-purpose warm relocate solutions.

The variationsin$f', \theta\ and\ \phi$ allocations used for dissimilar ideals of *Nt* is drawn within Diagram11-13. as of Diagram11 we examined to facilitate a ascend in *Nt*, slow downs the swiftness side view within the border line sheet system. This is since of the reality so as to as the values of *Nt* ampliflies the hydrodynamic border line sheet width is condensed. It is seen on or after facts12&13 so as to together $\theta\ and\ \phi$profiles lift up in the border line layer province meant for the elevated ideals of *Nt*. We perceived on or after diagram12 so as to the hotness differentiation are little, this is since of the detail so as to thermo phoretic limitation is a nanoscale parameter so that its authority is moderately fewer.

The consequence of heat/thermal emission constraint (*An*) on swiftness, hotness and focus side view is exposed in diagrams14-16. The swiftness side view amplify all the way from side to side the border line sheet by means of ampliflied in the power of thermal energy constraint(*An*)(Fig.14). It is observed structure Drawing15 so as to, the thermal border line sheet width is superior by way of the elevated ideals of *An* in the whole stream section. This is owing to the information so as to impressive thermal/hotness emission keens on the stream heater the solution, which origins intensification during the warmth of the explanation. though, present is a decelaration in the focus border line sheet width with mounting ideals of *An* as exposed in drawing16.

The allotment of$f', \theta\ and\ \phi$ for diverse ideals of Q are exemplify in Diagram17-19. Diagram17 disclose that the width of the impetus border line coating is superior by means of increasing ideals of heat source factor$(Q > 0)$, though, the side view of f' depreciates withheat incorporation constraint $Q < 0$. It is experiential that hotness in hot/thermal border line sheet amplify through the amplify in heat production constraint $Q > 0$, whereas,the profile of θ slow down with the warmth combination limitation $Q < 0$ as exposed in drawing18. This is due to the truth so as to, mounting the ideals of $Q > 0$ in the border line layer section generate power as a consequences hotness of the fluid enhances, where as lessening the ideals of $Q < 0$ suck up the hotness of the solution and is origins the deceleration within the hotness of the solution. though, the comparable conflicting leaning is perceived in the focus allocation by means of admiration to heat source/sink constraint (Q) in the solution section diagram19.

The shock of Lewis amount (*Le*) on impetus, heat/thermal and solutal border line coating thicknesses is plotted in drawing20-22. It is appeal noting at this occasion that an ampliflied in the assessment of Le leads to ampliflied the swiftness profiles in the border line coating governmentDrawing20. On the other hand, the hotness and focus allocation are together decelerate with rising ideals of Le. This is since of thereality that Lewi''s integer correspond to the quotient of thermal disseminatibity to the mass diffusivity. escalating the Lewi''s digit way lower themass diffuseivity causes the thinner concentration boundary layer.

Drawing 23-25 exemplified the consequence of resilience ratio parameter (*Nr*) on velocity, temperature and concentration distributions through the boundary layer regime. It is perceived since graph 23 so like to the size of hydrodynamic boundary line coating is condensed by means of enhancing values of*Nr*. It is seen as of Drawing24 to the hotness outline of the solution amplifies by means of mounting ideals of*Nr*. This is as of the certainty so as to elevated the price of resilience proportion constraint improves the solutions hotness, so as to the thermal border line coating width is augmented. The focus side sight amplifies all the mode from side to side the explanation segment for unrelated principles of*Nr*. (As in in Fig25).

The impact of themixed convection number parameter (*Ra*) on velocity, hotness and focus outlines conspired inside drwings26to28. An amplify in *Ra* enhanced the swiftness sharing (Drrawing26). It is scrutinized so as to in cooperation hotness as well as focus outline slow down through the escalating ideals of Ra. This is since the reality so as to resilience relative amount constraint (*Nr*) authority is fewer in the border line sheet administration than the diverse convection limitations, as a result so as to, in attendance is holding back within the breadth of thermal and solutal border line sheet. additionally, the hotness as well as focus side view amplify's asRa = 0 (enforced convection) as of no cheerfulness service, as well as together profiles retards through the escalating ideals ofRa.

The ideals of C_f, Nu_x as well as $Sh_x$for diverse ideals of the non-dimensional parameters is recognized in slab2- 6.

It is stated that the rates of swiftness as well as tempo collection relocate grow weaker in the solution management as the standards of *M*rises, on the other hand, rate's of warmth relocation accumulaites by way of the optimizing ideals of*M*. The C_f,Sh_x convoluted through scrambled ideals of *Ra*. on the other hand, the ideals of Nu_x degeneratewith progressede ideals of *Ra*and is exposed into box second.

The measurementless tariff swiftness $(-f'(0))$, rates of warmth relocation $(-\theta'(0))$ and rates of accumulation relocate $(-\phi'(0))$ for dissimilar ideals of warmth basis/go under constraint (Q) as well as wormth emission constraints (*An*) are pointed up in board3. It is expressed starting this board to the C_f along with Nu_xdegenerates by way of advancement ideals of warmth cause/go under constraint(Q), on the other hand, the Sh_x weakens by way of getting better ideals of warmth foundation/go down constraint(Q). It is too distinguished on or after this board so as to theC_f and Nu_xdeclines, while, the Sh_xboosted among mounting ideals of*An*.

The upshot of *Nb&Nt* lying on C_f,Nu_x&Sh_x be obtainable during board4. It's pragmatic on or subsequent to this board so as to the values ofC_f, $Nu_x$are in cooperation decelerates in the entire fluid regime with higher values of*Nb*, whereas,Sh_xvalues escalatewith improving ideals of *Nb*. It is moreover discovered on or after this board so as to the $C_f$values gain, howevierNu_x and Sh_x signifies degenerate in the fluid regime with higher values of *Nt*.

It's scrutinized so as to the C_f, *Shx ideals* diminishes in the full solution organization by way of escalating ideals of α, however, the Nu_xvalues upsurges with rising values of α. The ideals of C_f and Nu_x are upgrades with escalating values of*Nr,* anywhere, Sh_x diminishes with elaborating ideals of *Nr*and is offered within board5.

The swayof Lewi's integer (*Le*) lying on C_f,Nu_x as well as Sh_x is grouping in board The ideals of C_f&$Nu_x$are bothdeteriorate with an percentage amplify in the assessment of *Le* during the entire boundary sheet province. However, the ideals of Sh_xupgrade in the solution administration by way of mounting ideals of *Le*.

5. 5. Wrapping up

within this commentary, a conjectural revision is put into operation to scrutinize the warmth as well as accumulation relocate distinctiveness ofMHD nanofluidalong an disposed upright shield implanted within permeable middling by way of thermal emission along with warmth engender starting place. The side view of swiftness, warmth as well as focus since well asreduced Nussalt and Sherewood numberswere premeditated for unlike ideals of essential constraints. The places of interest of the in attendance dilemma can be recapitulate as pursued.

i) Temperature and concentration side views mounts by way of superior ideals of(*M*). on the other hand, the ramp of hotness develops but the gradiaent of dissemination slow downs among ever-increasing ideals of*M*.

ii) in cooperation constraints*Nb* and *Nt*decelerates the depth of the thermal border line deposit in the stream province.

iii) escalating the shield penchant position(α) put on a pedestal the hotness as well as focus allotments.

iv) hotness side views augments through escalating ideals of *An*, but the measurement a smaller sum temperatureand collection relocate toll augments with*An*.

v) warmth side views lifts up through warm production constraint Q> 0, but retards by way of warmth assimilation constraint Q< 0

Table 1: Comparison of $-\theta'(0)$ and $-\phi'(0)$ with PuneetRana etal [22] for Nr=0.5, Ra=1.0, α = π/6 and M=0, An=0, Q=0.

Parameter			$-\theta'(0)$		$-\phi'(0)$	
Le	Nb	Nt	PuneetRana et al. [22]	Present Study	PuneetRana et al. [22]	Present Study
5.0	0.5	0.1	0.4425	0.4429	1.5101	1.5103
5.0	0.5	0.3	0.4064	0.4065	1.5106	1.5107
5.0	0.5	0.5	0.3742	0.3744	1.5194	1.5196
5.0	1.0	0.1	0.3025	0.3026	1.5433	1.5433
5.0	1.0	0.3	0.2779	0.2780	1.5601	1.5603
5.0	1.0	0.5	0.2559	0.2561	1.5803	1.5804
5.0	1.5	0.1	0.0879	0.0880	1.5693	1.5695
5.0	1.5	0.3	0.0807	0.0809	1.5855	1.5856
5.0	1.5	0.5	0.0742	0.0744	1.6013	1.6015
15	0.5	0.1	0.4298	0.4299	2.6943	2.6945
15	0.5	0.3	0.3933	0.3936	2.7160	2.7165
15	0.5	0.5	0.3609	0.3609	2.7461	2.7464
15	1.0	0.1	0.2823	0.2825	2.7192	2.7196
15	1.0	0.3	0.2579	0.2580	2.7444	2.7449
15	1.0	0.5	0.2366	0.2366	2.7741	2.7745
15	1.5	0.1	0.0747	0.0749	2.7362	2.7364
15	1.5	0.3	0.0683	0.0683	2.7555	2.7559
15	1.5	0.5	0.0626	0.0626	2.7735	2.7740

Table 2: The effect of magnetic parameter (*M*) and Rayleigh number (*Ra*) on skin- friction coefficient$\left(-f'(0)\right)$ local Nusselt number $\left(-\theta'(0)\right)$ and local Sherwood number $\left(-\phi'(0)\right)$for fixed Q=0.2,Nr=0.5, An=0.5, Nb=0.5, Nt=0.5, $\alpha = \pi/_6$, Le=10.

M	***Ra***	C_f	Nu_x	Sh_x
0.1	0.5	0.25272	0.72901	0.82377
0.3	0.5	0.15268	0.75646	0.41532
0.5	0.5	0.12914	0.77888	0.19075
0.7	0.5	0.12184	0.79367	0.06651
1.0	0.5	0.11637	0.80319	0.00792
0.5	0.1	0.13533	0.74269	0.57139
0.5	0.3	0.19594	0.73543	0.69702
0.5	0.5	0.25272	0.72900	0.82379
0.5	0.7	0.30671	0.72359	0.94944
0.5	1.0	0.33819	0.72082	1.02365

Table 3: The effect of heat source/sink parameter (*Q*) and thermal radiation parameter (*An*) on skin- friction coefficient$\left(-f'(0)\right)$ local Nusselt number $\left(-\theta'(0)\right)$ and localSherwood number $\left(-\phi'(0)\right)$for fixed M=0.5, Nr=0.5, Ra=0.5, Nb=0.5, Nt=0, $\alpha = \pi/_6$, Le=10.

Q	***An***	C_f	Nu_x	Sh_x
0.5	0.5	0.25272	0.72900	0.82379
0.2	0.5	0.27391	0.91357	0.67754
0.0	0.5	0.28945	1.07519	0.53667
-0.1	0.5	0.30169	1.22119	0.40145
-0.3	0.5	0.31175	1.35562	0.27160
0.2	0.1	0.29860	1.20284	0.41403
0.2	0.2	0.29305	1.14475	0.46572
0.2	0.3	0.28800	1.09485	0.50887
0.2	0.4	0.28336	1.05131	0.54548
0.2	0.5	0.27906	1.01286	0.57696

Table 4: The effect of Brownian motion parameter (*Nb*) andthermophoresisparameter (*Nt*) on skin- friction coefficient$\left(-f'(0)\right)$, local Nusselt number $\left(-\theta'(0)\right)$ and local Sherwood number $\left(-\phi'(0)\right)$for fixed M=0.5, Nr=0.5, Ra=0.5, Q=0.2, An=0.5, $\alpha = \pi/_6$, Le=10.

Nb	***Nt***	C_f	Nu_x	Sh_x
0.1	0.5	0.26525	0.75211	0.56167
0.3	0.5	0.25297	0.67875	0.74299
0.5	0.5	0.24460	0.61327	0.82215
0.7	0.5	0.23775	0.55505	0.86516
1.0	0.5	0.23174	0.50344	0.89125
0.5	0.1	0.25970	0.81386	0.84588
0.5	0.3	0.26263	0.78034	0.69553
0.5	0.5	0.26262	0.75213	0.56151
0.5	0.7	0.26765	0.72602	0.44185
0.5	1.0	0.27075	0.69034	0.28556

Table-5: The effect of inclination angle (α) and buoyancy ratio parameter (*Nr*) on skin- friction coefficient$\left(-f'(0)\right)$ local Nusselt number $\left(-\theta'(0)\right)$ and local Sherwood number $\left(-\phi'(0)\right)$for fixed M=0.5, Ra=0.5, Q=0.2, An=0.5, Le=10, Nb=0.5, Nt=0.5.

α	***Nr***	***C***		

α	Nr	C_f	Nu_x	Sh_x
0	0.5	0.26967	0.72721	0.86287
$\pi/6$	0.5	0.25272	0.72900	0.82379
$\pi/4$	0.5	0.23226	0.73125	0.77730
$\pi/3$	0.5	0.20495	0.73438	0.71663
$\pi/2$	0.5	0.13533	0.74269	0.57139
$\pi/6$	0.0	0.34581	0.72303	0.92679
$\pi/6$	0.25	0.28299	0.72677	0.87687
$\pi/6$	0.5	0.22336	0.73154	0.76829
$\pi/6$	0.75	0.16821	0.73774	0.64847
$\pi/6$	1.0	0.14295	0.74160	0.58321

Table 6: The effect of Lewis number (Le)on skin- friction coefficient$\left(-f'(0)\right)$, local Nusselt number $\left(-\theta'(0)\right)$ and local Sherwood number $\left(-\phi'(0)\right)$for fixed M=0.5, Nr=0.5, Ra=0.5, Q=0.2, An=0.5,$\alpha = {}^{\pi}/_{6}$, Le=10.

Le	C_f	Nu_x	Sh_x
10	0.26525	0.75211	0.56169
12	0.25935	0.74167	0.67414
14	0.25470	0.73290	0.77604
16	0.25092	0.72538	0.86971
19	0.24775	0.71881	0.95672

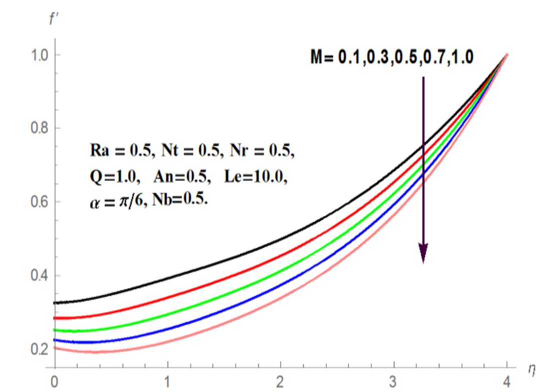

Fig.2. The effect of (M) on velocity profiles.

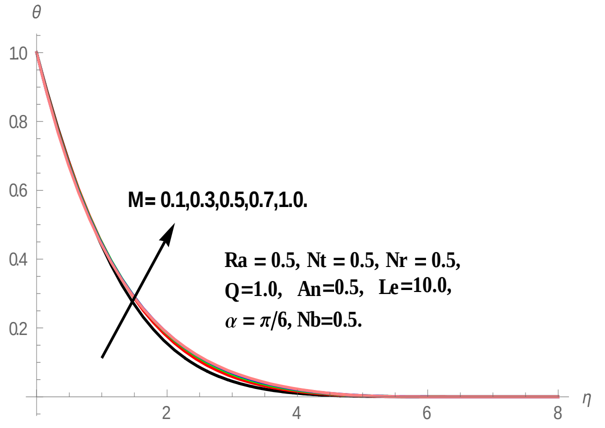

Fig.3. The effect of (M) on Temperature profiles.

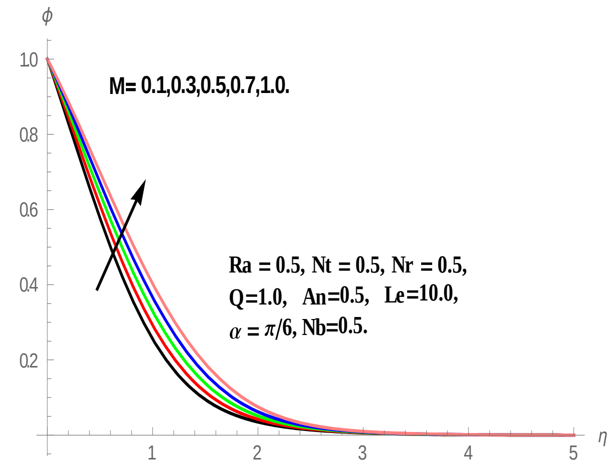

Fig.4. The effect of (M) on Concentration profiles**.**

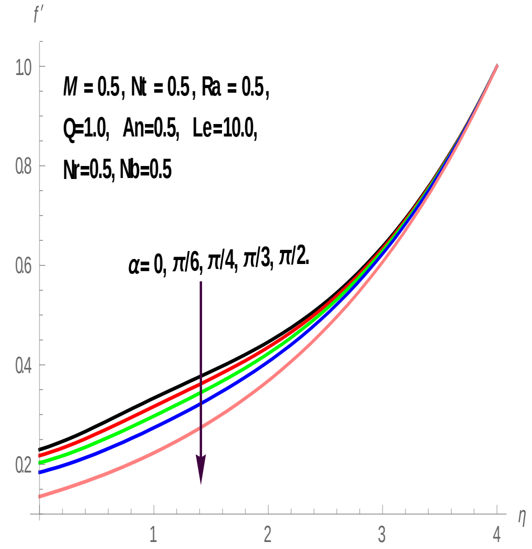

Fig.5. The effect of (α) on velocity profiles**.**

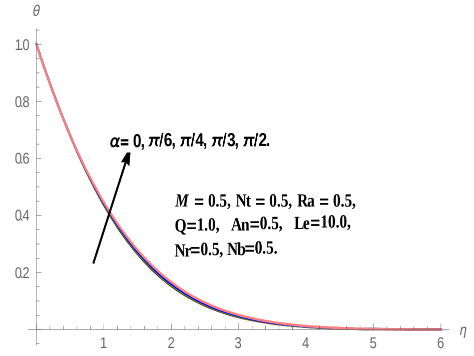

Fig.6. The effect of (α) on Temperatureprofiles.

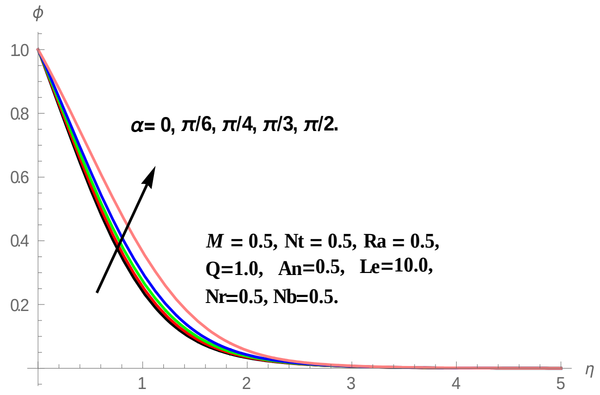

Fig.7. The effect of (α) on Concentration profiles**.**

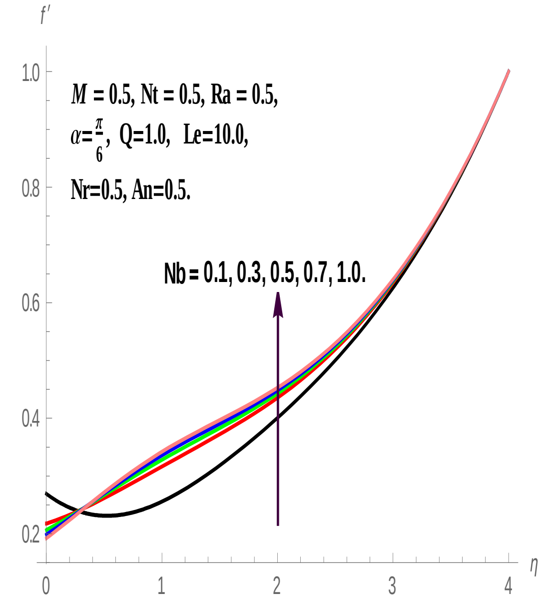

Fig.8. The effect of (*Nb*) on velocity profiles.

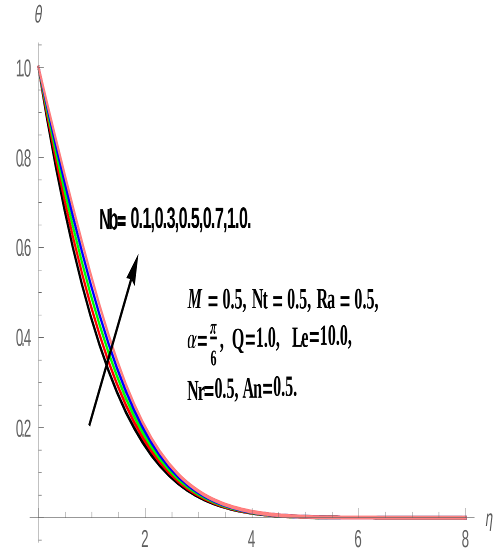

Fig.9. The effect of (Nb) on Temperature profiles.

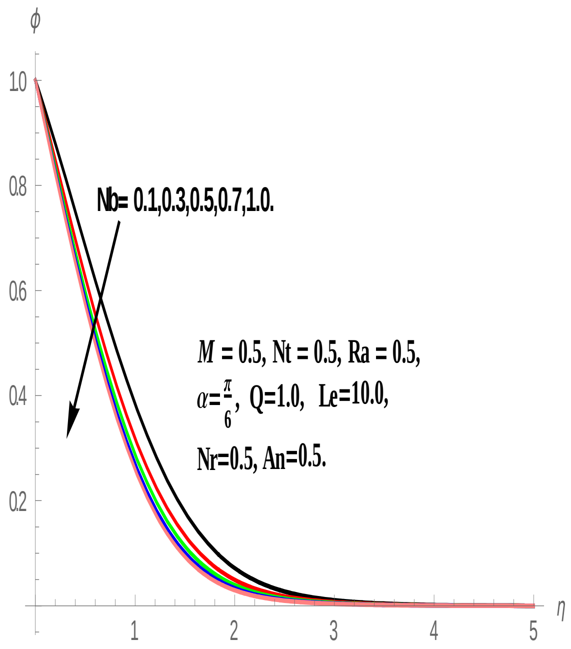

Fig. 10. The effect of (Nb) on Concentration profiles.

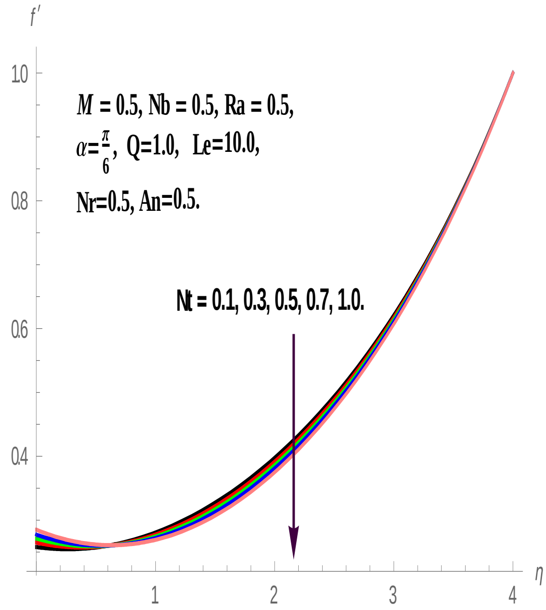

Fig.11. The effect of (Nt) on velocity profiles**.**

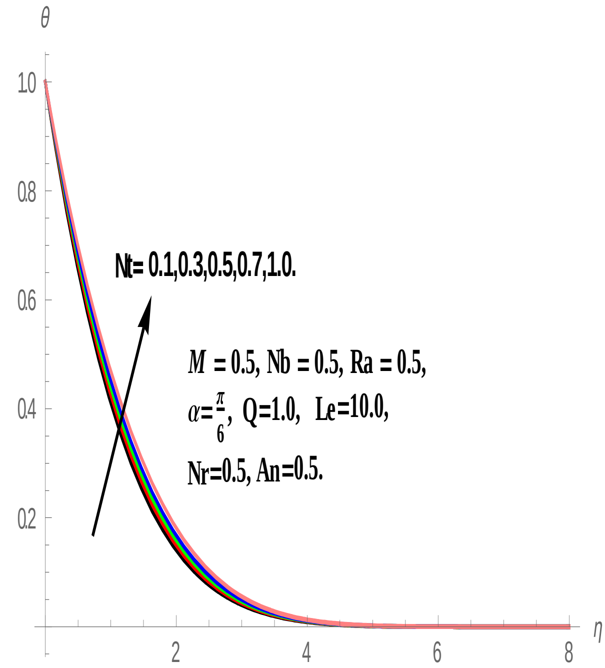

Fig.12. The effect of (Nt) on Temperature profiles**.**

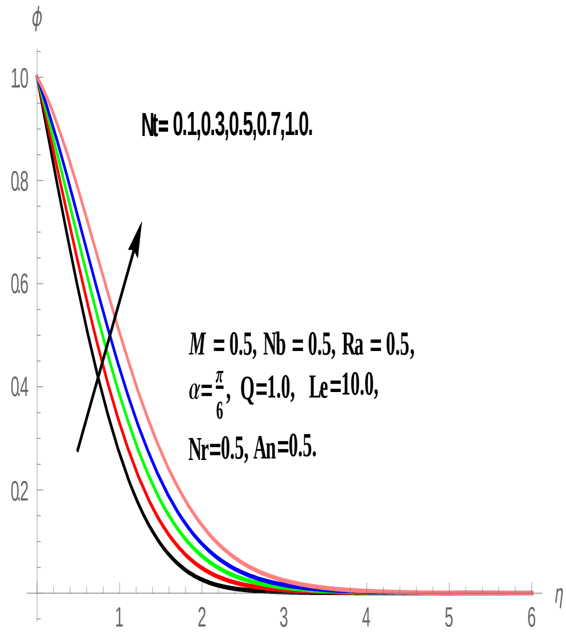

Fig.13. The effect of (Nt) on Concentration profiles.

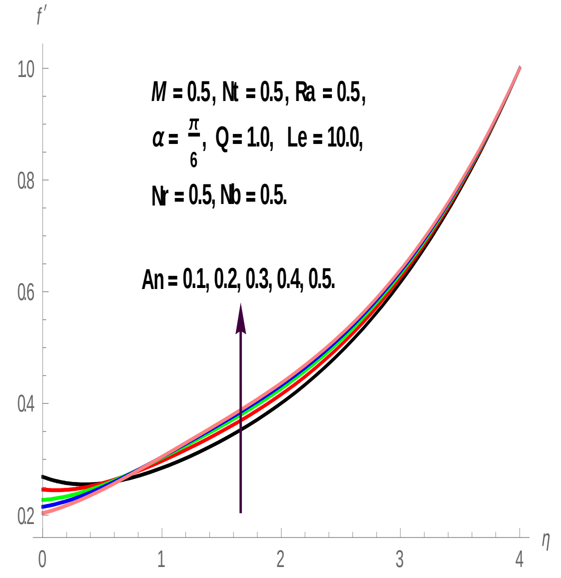

Fig. 14. The effect of (*An*) on Velocity profiles**.**

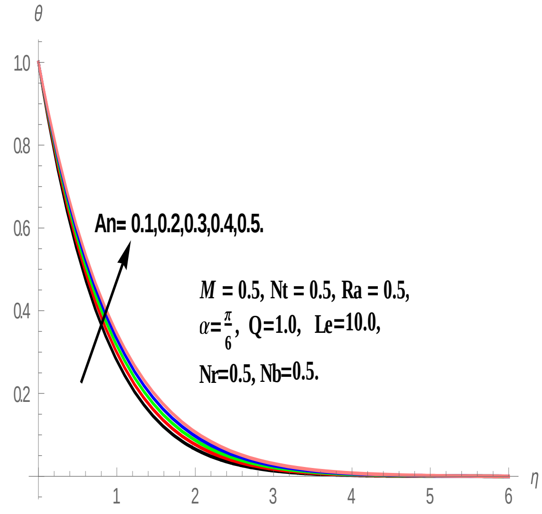

Fig.15. The effect of (*An*) on Temperature profiles.

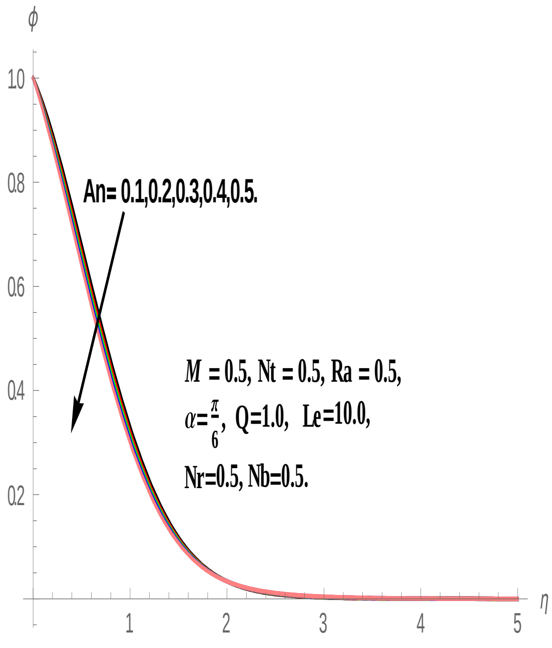

Fig. 16. The effect of (An) on Concentration profiles.

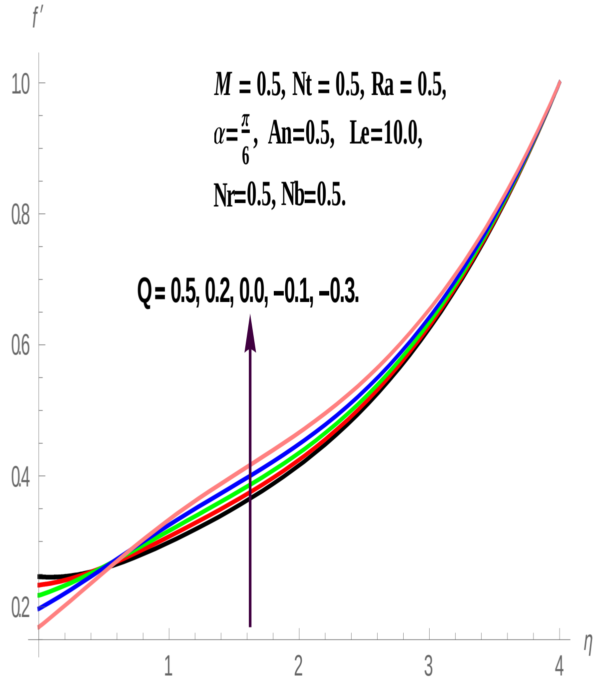

Fig.17. The effect of (Q) on Velocity profiles.

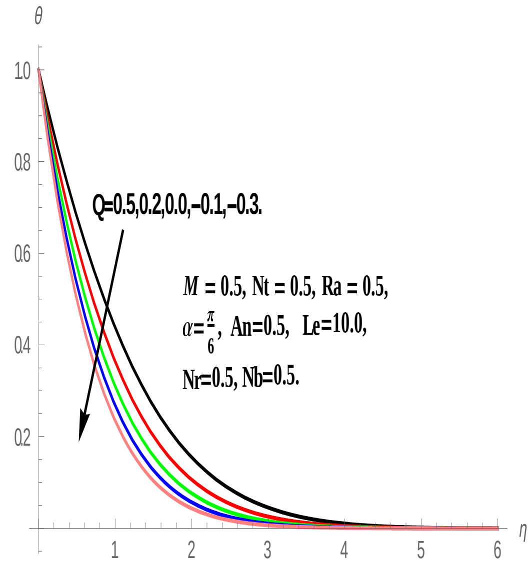

Fig.18. Theeffect of (Q) on Temperature profiles.

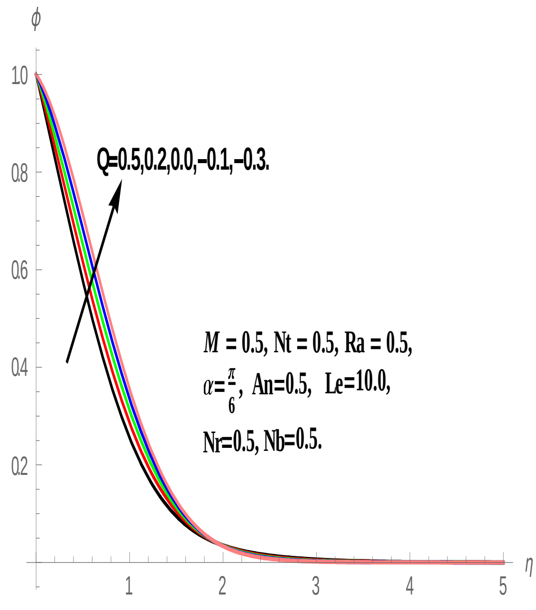

Fig.19. The effect of (Q) on Concentration profiles.

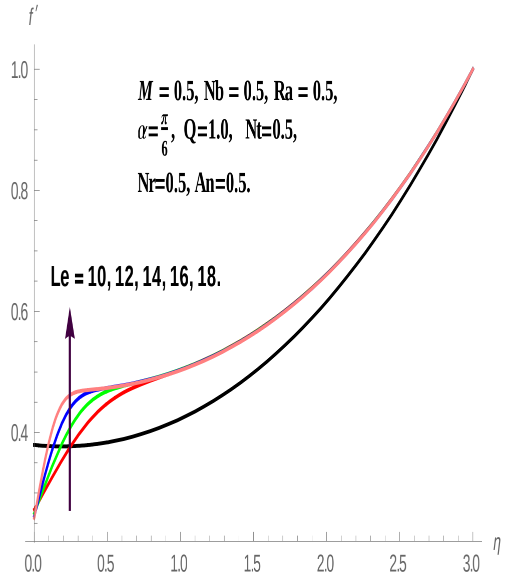

Fig.20. The effect of (*Le*) on Velocity profiles.

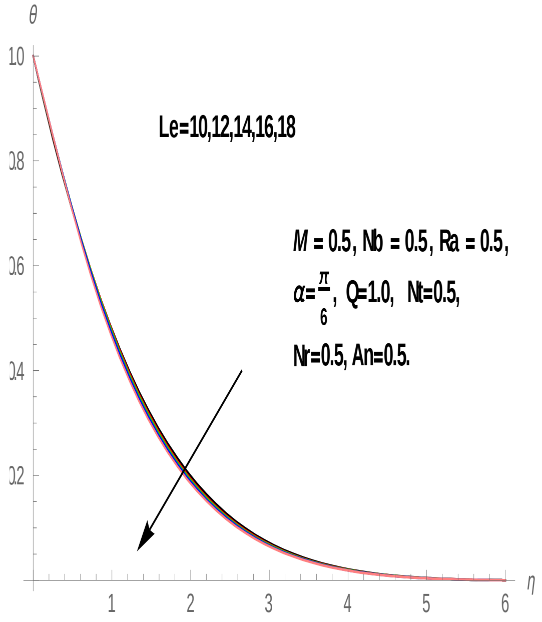

Fig.21. The effect of (*Le*) on Temperature profiles.

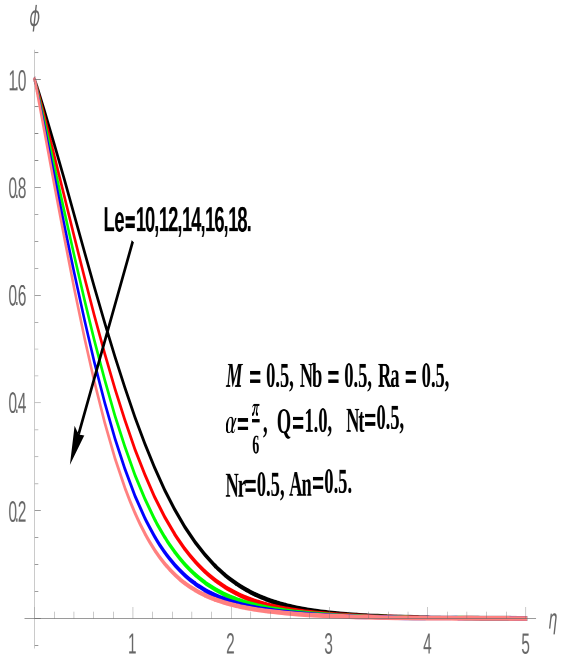

Fig.22. The effect of (*Le*) on Concentration profiles.

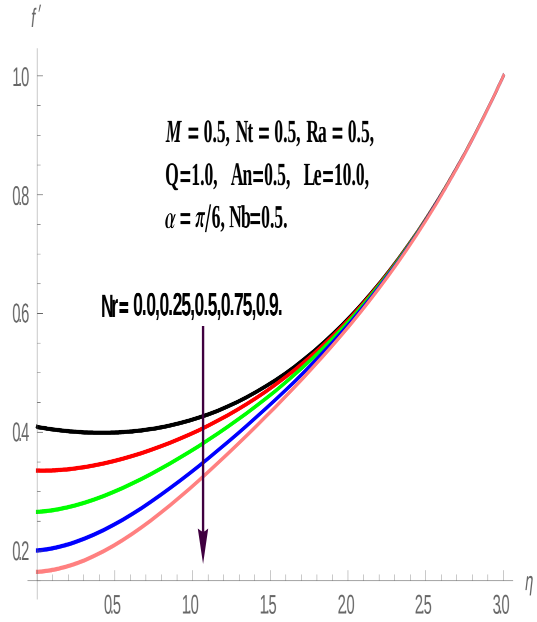

Fig.23. The effect of (*Nr*) on Velocity profiles**.**

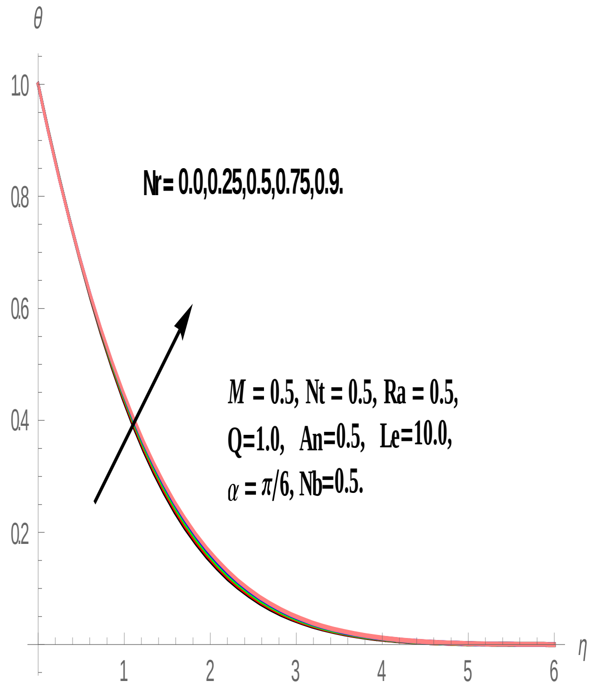

Fig.24. The effect of (*Nr*) on Temperature profiles.

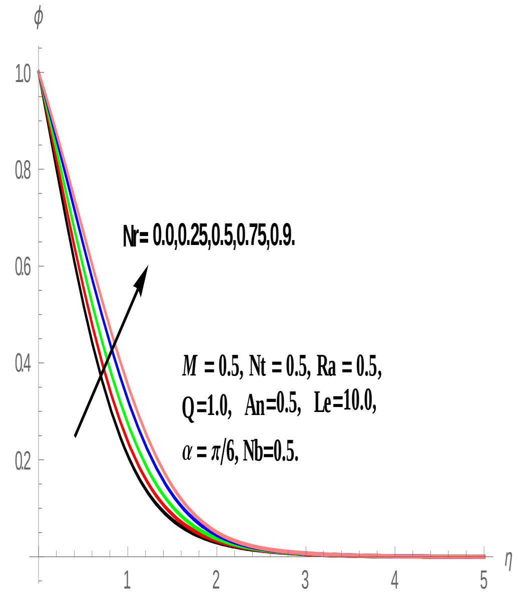

Fig.25. The effect of (*Nr*) on Concentration profiles.

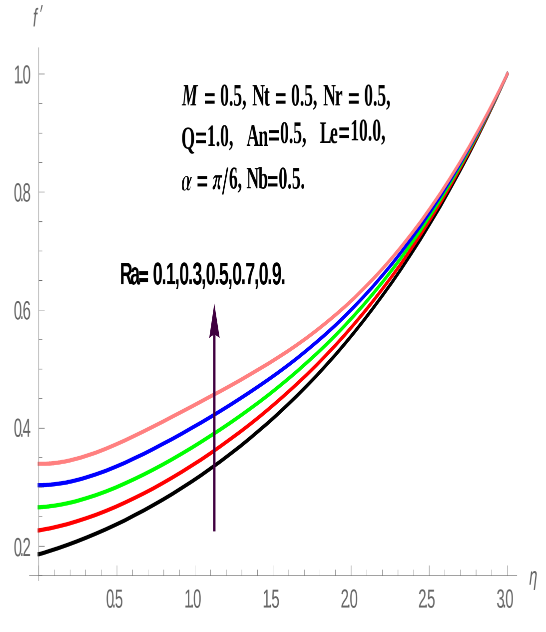

Fig.26. The effect of (*Ra*) on velocityprofiles**.**

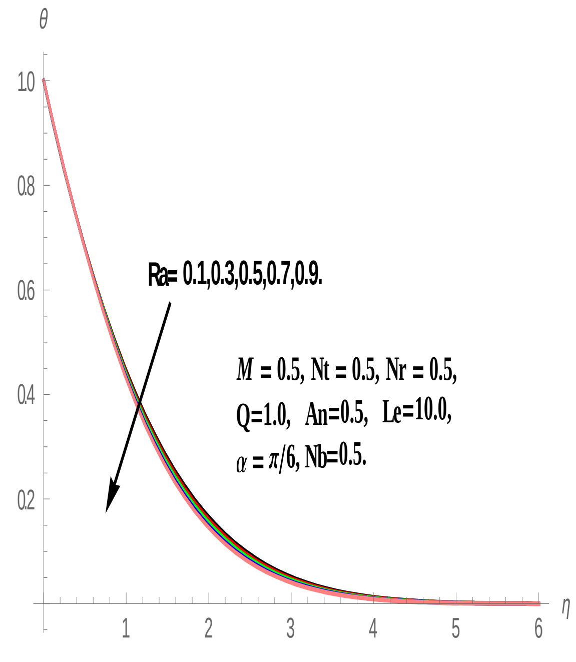

Fig.27. The effect of (*Ra*) on Temperature profiles**.**

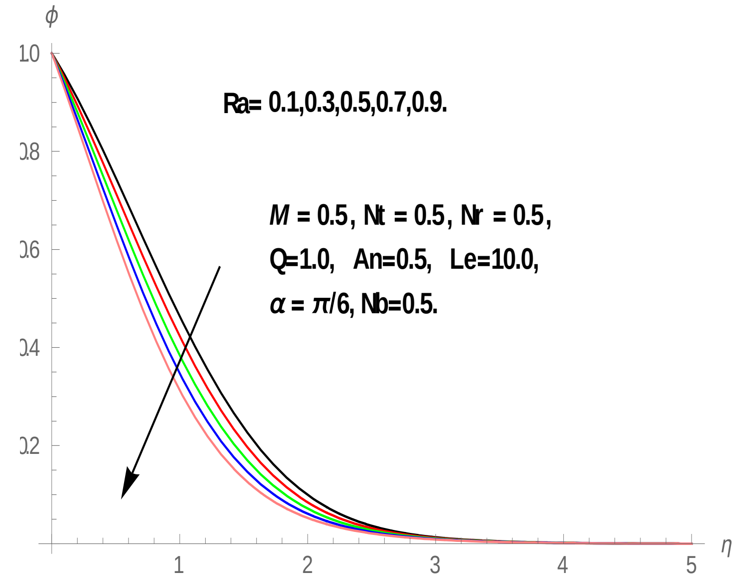

Fig.28. The effect of (*Ra*) on Concentration profiles**.**

Nomenclature

G Gravitational acceleration vector
K_m Thermal conductivity
C Nanoparticle volume fraction
C_∞ Ambient nanoparticle volume fraction
T_w Temperature at the plate
T Temperature on the plate
q_w Wall heat flux
D_B Brownian diffusion
$f(\eta)$ Dimensionless stream function
Nt Thermophoresis parameter
P Pressure
W Darcy velocity (u, v)
M Magnetic parameter

Ra Mixed convention parameter
Nu Nusselt number
C_w Nanoparticle volume fraction on the plate
(x, y) Cartesian coordinates
T_∞ Ambient temperature attained
$\frac{Ra_x}{Pe_x}$ Mixed parameter coefficient
q_m Wall mass flux
D_T Thermophoretic diffusion coefficient
g Gravitational acceleration
Le Lewis number
Nb Brownian motion parameter
q''' Thermal radiation
Q Heat source parameter

Greek symbols

μ viscosity
κ permeability of porous medium
ρ_f Fluid density
ψ Stream function
τ Parameter defined by $\varepsilon \frac{(\rho c)_p}{(\rho c)_f}$
ϕ (η) Dimensionless nanoparticle volume fraction
θ (η) Dimensionless temperature
α Acute angle of the plate to the vertical

ε porosity
α_m Parameter defined by $\frac{k_m}{(\rho c)_f}$.
ρ_p Nanoparticle mass density
V Kinematic viscosity of the fluid
$(\rho c)_f$ Heat capacity of the fluid
η Similarity variable
$(\rho c)_p$ Effective heat capacity of the nanoparticle
β Volumetric expansion coefficient

Subscripts

w Condition on the plate
∞ Condition far away from the plate
η Similarity variable
f Base fluid.

References